

**EPTT-2024-0042**  
**TURBULENCE CHARACTERISTICS ANALYSIS IN HORIZONTAL OIL-  
WATER CORE-ANNULAR FLOW VIA PARTICLE IMAGE  
VELOCIMETRY (PIV).**

**J. E. Arrollo-Caballero**

**P. J. Miranda-Lugo**

**O. M. H. Rodriguez**

University of São Paulo (USP), São Carlos School of Engineering (EESC), Mechanical Engineering Department, Industrial Multiphase Flow Laboratory (LEMD), Av. Trab. São Carlense, 400 - Parque Arnold Schmidt, São Carlos - SP, 13566-590, Brazil.  
[jorgearrollo@usp.br](mailto:jorgearrollo@usp.br), [pjosemiranda@usp.br](mailto:pjosemiranda@usp.br), [oscarmhr@sc.usp.br](mailto:oscarmhr@sc.usp.br) .

**Abstract.** *The oil-water core-annular flow pattern is characterized by the configuration in which the more viscous fluid occupies the core of the pipe, and the less viscous fluid forms a ring around the core, maintaining contact with the pipe wall. It has been suggested as a means of transporting or artificially lifting high-viscous oils since it minimizes frictional pressure drop. Previous studies have shown that the transition and stability phenomena of the core-annular flow pattern could be associated with the interfacial wave structure and the phases' turbulence. However, the information available in the literature on wave amplitude, wavelength, and turbulence statistics is limited, especially for liquid-liquid systems. This study aims to characterize the hydrodynamic behavior of the core-annular flow, obtaining the axial and radial velocity distributions, as well as its turbulent characteristics, such as  $U_{rms}$ ,  $V_{rms}$ , and Reynolds stress. Experiments were carried out in a borosilicate glass tube with an internal diameter of 9.7 mm using the PIV technique. The PIV methodology allowed to obtain the detailed hydrodynamics of the core-annular flow by acquiring 3000 frames in the pipe's diametral plane, and the interface's height using the PLIF technique. A noticeable change in the axial velocity profile was observed near the interface at the top of the tube, suggesting a possible instable hydrodynamic condition. In addition, the increase in mixture velocity directly impacted the magnitude of  $U_{rms}$  and  $V_{rms}$ , reflecting an increase in turbulence in the flow. The Reynolds stresses were examined under different experimental conditions, revealing a characteristic behavior of the annular flow pattern in the turbulent shear stress data, especially at the interface region at the top of the tube.*

**Keywords:** *Core-annular flow, Oil-water flow, PIV, Turbulence statistic, Velocity profiles.*

## 1. INTRODUCTION

Flows of non-miscible fluids are found in nature and various industrial equipment, such as air conditioning systems, refrigeration, nuclear power plants, and chemical processing. Different spatial configurations, called flow patterns, can be adopted when such fluids flow simultaneously in a pipe. Three main groups are found in the literature: dispersed, intermittent, and separated flows. In the latter, annular and stratified flow patterns are found, where the phases separate into distinct continuous layers. (Brauner, 1991; Rodriguez & Bannwart, 2008). Core-annular flow has been used to transport highly viscous fluids in industrial applications. This flow type has become attractive due to the reduction in pressure drop in liquid transportation lines. The less viscous fluid forms a ring around the more viscous fluid, avoiding contact between the latter and the pipe wall, which results in lower flow resistance.

Many experimental studies have focused on the measurement of the hydrodynamic characteristics of core-annular flow in horizontal and inclined pipes; Sutharshan, 1995; Bannwart, 2001; Bannwart et al., 2004; Rodriguez & Bannwart, 2006; Zadrazil et al., 2014; Zadrazil & Markides, 2014; Ashwood et al., 2014; Shi & Yeung, 2017. Sutharshan (1995) used a photochromic dye activation technique to study the mechanism of liquid transport around the inner perimeter of a pipe in horizontal core-annular flow. Experiments were conducted in a 5.28 m long horizontal pipe with an internal diameter of 25.4 mm, using air and kerosene at near atmospheric pressure conditions. That author measured liquid film velocities in radial and axial directions in a non-invasive manner. It was revealed that the spot dye trace moved upward indicating the transport of liquid in an upward direction against the force of gravity during the passage of periodic disturbance waves. These findings suggest that liquid transport to the top of the pipe occurs mainly due to disturbance waves, and not by other mechanisms, as previously suggested.

Zadrazil and Markidez (2014) experimentally characterized downward vertical annular gas-liquid flow using PIV, PTV, and PLIF simultaneously. The conditions investigated covered a wide range of liquid and gas Reynolds numbers. They obtained information on the local and instantaneous velocity fields under interfacial waves, identifying recirculation zones within the liquid films under certain conditions, as well as mean velocity profiles, RMS velocity fluctuation, and kinetic energy of the liquid films.

In this study we analyze the turbulence characteristics of a horizontal oil-water core-annular flow via the 2-D PIV technique and the interface height using the PLIF technique (the latter was only used to indicate interface position, and the details were not included in the scope of this paper). The instantaneous local velocity was measured and the mean axial and radial velocity components were calculated, as well as the velocity fluctuations and Reynolds stresses.

## 2. EXPERIMENTAL WORK

### 2.1. Experimental setup

The experimental campaign was carried out in a new experimental facility for studying liquid-liquid two-phase flows at the Industrial Multiphase Flow Laboratory (LEMI), see Fig. 1. The working fluids were water ( $998 \text{ kg/m}^3$ ) and mineral oil ( $805 \text{ kg/m}^3$ ), with an interfacial tension  $\sigma = 20.79 \text{ mN/m}$  and a viscosity ratio of  $\mu_o/\mu_w = 1.44$ . The rig consists of two independent supply lines for water and oil and two test sections (F and K) made of borosilicate glass tubes with lengths ( $L_p$ ) of 4.5 and 7.5 m and internal diameters (i.d.) of 9.7 and 20.5 mm, respectively. Each test section has a rectangular transparent acrylic viewing section (G and L), where the PIV system is installed. The fluid distribution system is driven by positive displacement hydraulic pumps from two reservoirs (A and B). The fluids are injected into the test section through flow rectifiers (C, D, H, and I) and a specially designed inlet section (E and J). The former aims to reduce the large-scale structures of the flow at the entrance to the test section, while the latter prevents the liquids from mixing inside the test section and promotes a separate flow. Both flow lines have a set of liquid flow meters (1, 2, 4, 5), K-type thermocouples (3, 6, 7, 8) and differential pressure transducers (9, 10). The two-phase mixture from the test section is pumped to an oil-water separator (M). From this separator, each fluid is transported to the reservoirs (N and Q) and then pumped by positive displacement pumps (P and S), controlled by variable frequency controllers (O and R), to their respective reservoirs (A and B), completing the test loop.

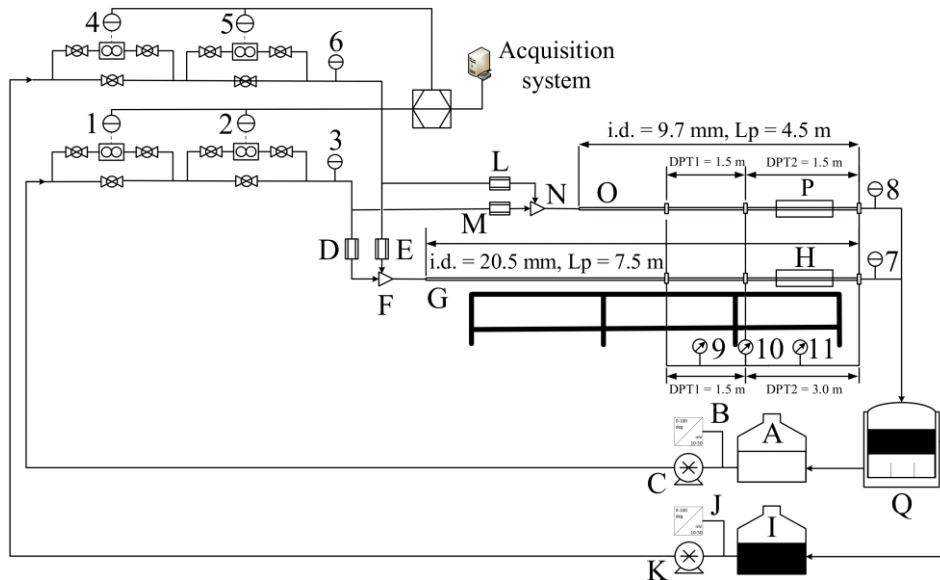


**Figure 1.** Schematic representation of the liquid-liquid test facility at the Industrial Multiphase Flow Laboratory (LEMI).

### 2.2 Experimental procedure

The oil ( $J_1$ ) and water ( $J_2$ ) superficial velocities were defined using a flow pattern map obtained experimentally by varying the fluid velocities and identifying the region where the annular flow was observed; see Fig. 2.. Table 2 shows the experimental flow conditions, as well as the phases' holdup and Reynolds numbers calculated considering the superficial velocity. The hydraulic diameter was defined from the information obtained from the mean interface height, measured via PLIF. It is also important to note that, despite the region appearing somewhat broad, only six experimental

points could be analyzed. At those points, the annular flow was sufficiently stable and did not exhibit significant phase dispersion (Arrollo Caballero, 2023).

The instantaneous local velocity were measured, the mean axial and radial velocity components, and the velocity fluctuations and Reynolds stresses were calculated via PIV technique.

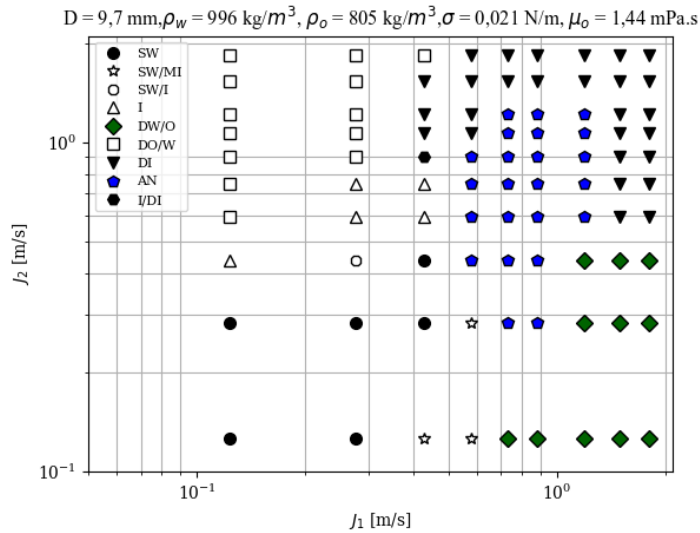


**Figure 2.** Flow pattern map. DI(dispersed), AN(annular), DW/O (dispersion of water in oil), DO/W(dispersion of oil in water, I(Intermittent), MI( mixture at the interface), SW(wavy stratified), I/DI (Intermittent with dispersion), SW/MI(wavy stratified with mixture at the interface), SW/I(wavy stratified with Intermittent transition).  $J_1$  represents the oil superficial velocity while  $J_2$  is the water superficial velocity.

**Table 2.** Experimental conditions for each experimental point, mixture velocity ( $J_m$ ), water cut ( $\epsilon_2$ ), superficial Reynolds of oil and water ( $J_1$  and  $J_2$ ) and frames per acquisition.

#	$J_1$ (m/s)	$J_2$ (m/s)	$J_m$ (m/s)	$\epsilon_2$ (-)	$Re_{sw}$ (-)	$Re_{so}$ (-)	# Frames
1	0.58	0.59	1.17	0.51	3685	2962	3000
2	0.64	0.62	1.26	0.49	3878	3273	3000
3	0.64	0.65	1.29	0.51	4072	3273	3000
4	0.64	0.68	1.32	0.52	4265	3273	3000
5	0.67	0.68	1.36	0.51	4265	3430	3000
6	0.73	0.72	1.48	0.51	4652	3740	3000

### 2.3 Data treatment and analysis

Figure 4 shows an original image recorded in a typical experiment by sync 2D-PIV and PLIF techniques. Despite the use of rhodamine, the particles are not opacified, providing a clear image of the particles and the interface. Those images were processed with a cross-correlation function using a multi-pass approach to obtain the velocity field. In the first two passes, which correspond to the initial estimation of the velocity vectors, an adaptive PIV interrogation window of 64 x 64 pixels was defined with an overlap of 50% in the adjacent areas. In the last two passes, the window was reduced to 24 x 24 pixels with an overlap of 25% to enhance the velocity field spatial resolution.

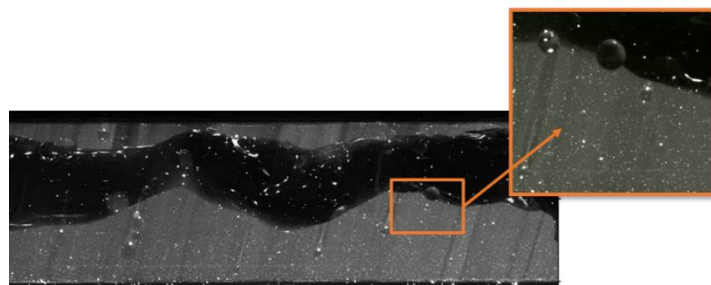


**Figure 4.** Original image recorded by the PIV camera. Showing water in the gray region and oil in the black region.

The instantaneous velocity data in the streamwise and radial direction obtained after applying the cross-correlation function were used to calculate the local time-average axial ( $U_{mean}$ ) and radial ( $V_{mean}$ ) velocity components according to Eqs. 1 and 2, respectively.

$$U_{mean} = \frac{1}{n} \sum_{i=1}^n u_i \quad (1)$$

$$V_{mean} = \frac{1}{n} \sum_{i=1}^n v_i \quad (2)$$

where  $n$  represents the number of instantaneous velocity data (number of images),  $u_i$  and  $v_i$  are the instantaneous local axial and radial velocity components, respectively. Equations 3 and 4 estimate the axial and radial standard deviation of the local velocity components, respectively, or the *rms* velocity fluctuation (root mean square).

$$U_{rms} = \sqrt{\frac{1}{n} \sum_{i=1}^n (u_i - U_{mean})^2} \quad (3)$$

$$V_{rms} = \sqrt{\frac{1}{n} \sum_{i=1}^n (v_i - V_{mean})^2} \quad (4)$$

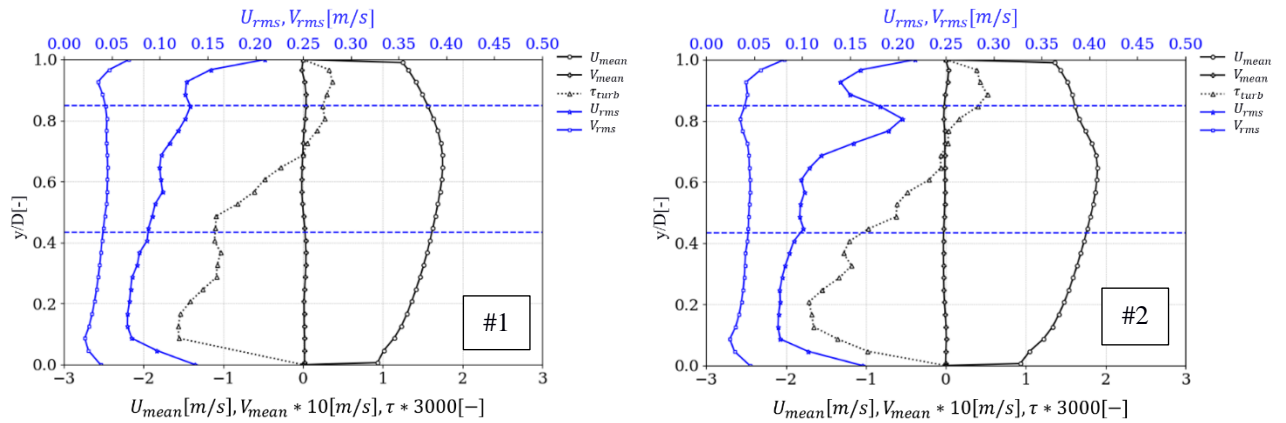
The cross-moments are defined by Equation 5. Here,  $u'$  and  $v'$  represent the components of the velocity fluctuation in the axial and radial directions. The Reynolds shear stress is obtained by multiplying by -1 and the liquid density the cross-moment given by Eq. 5. i.e.,  $-\rho \langle u' v' \rangle$ .

$$\langle u' v' \rangle = \frac{1}{n} \sum_{i=1}^n (u_i - U_{mean})(v_i - V_{mean}) \quad (5)$$

### 3 RESULTS AND DISCUSSIONS

Figure 6 represents the time averages of the axial ( $U_{mean}$ ) and radial ( $V_{mean}$ ) velocity profiles, the axial ( $U_{rms}$ ) and radial ( $V_{rms}$ ) velocity fluctuations, and the Reynolds stress ( $\tau_{turb}$ ) for each flow conditions evaluated in this study. The horizontal dashed blue lines represent the mean height of the top and bottom interfaces at the diametrical vertical plane of the flow, which was calculated using the interface position data obtained from the wave geometry analysis of PLIF data. This was done to calculate the Reynolds stress taking into account the corresponding fluid densities.

Diferently from single-phase flow, the location of the maximum axial velocity depends on the oil's core's position ( $U_{mean}$ ). It is interesting to see the relatively low velocity-gradient jumps at the oil-water interface, which can be explained due to low viscosity ratio (1.44), and the fact that both fluids are in turbulent regime with close Re numbers.



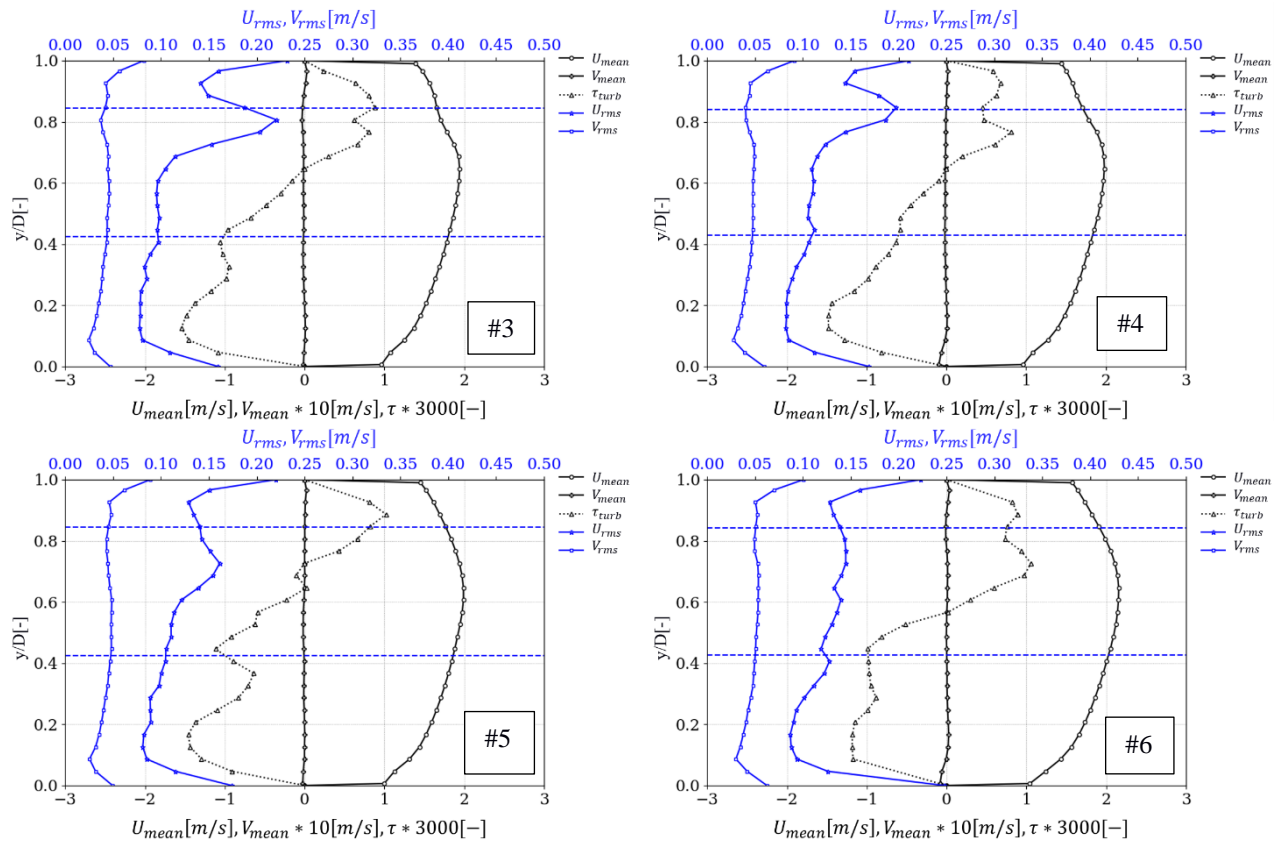


**Figure 6.** Mean radial and axial velocities and turbulence statistics for horizontal core-annular flow for each condition given in **Table 2**.

The radial velocity is near zero in all cases. The axial ( $U_{rms}$ ) and radial ( $V_{rms}$ ) velocity fluctuations have magnitudes about 5% and 15% of the axial velocity. However, the axial ( $U_{rms}$ ) velocity fluctuation presents a significant trend change near the top interface, a behaviour that might be related to a source of instability. The Reynolds stresses show trend changes at both interfaces' positions, which means that there is turbulence damping due to the presence of the interface. Authors such as Elseth (2001), Kumara et al. (2010), Ibarra et al. (2018), and Ibarra et al. (2021) reported similar results for stratified flow.

## 4 CONCLUSIONS

Understanding the dynamics of liquid-liquid core-annular flow is fundamental to advancing the knowledge of this flow pattern hydrodynamics stability. This study focuses on characterizing core-annular oil-water flow in a horizontal pipe using Particle Image Velocimetry (PIV-2D) and Planar Laser Induced Fluorescence (PLIF) techniques.

Experimental results revealed significant differences between single-phase and two-phase flow velocity profiles. In single-phase flow, the velocity profile is symmetric, while in annular flow this symmetry is lost, influenced by the position of the oil core. The velocity distribution in annular flow is similar to a turbulent profile due to the comparable properties of the fluids and their low viscosities, together with a close density and viscosity ratio and both in a turbulent regime.

The radial velocities are nearly zero, with slight fluctuations in the region where the interface position was estimated, indicating that inertial forces predominate over viscous effects. The Reynolds stress tensor analysis shows fluctuations in the areas where the axial velocity gradient fluctuates, related to the presence of the interfaces. It is also evident that the greater the Reynolds numbers, the higher the fluctuations related to turbulence ( $U_{rms}$  and  $V_{rms}$ ). Our results indicate that the oil core in core-annular flow plays a crucial role in modifying the axial velocity profile and turbulence statistics, introducing significant variations in the interfacial structure. This knowledge can be used to develop and validate advanced two-phase flow models in experimental applications.

## 5 ACKNOWLEDGEMENTS

The authors gratefully acknowledge National Council for Scientific and Technological (CNPq) for the grants of Jorge E. Arrollo-Caballero (proc. 131659/2021-9) and Oscar M. H. Rodriguez's (proc. 311057/2020-9) and CAPES (Coordination of the Improvement in Higher Level Personnel of Brazil) for Pedro J. Miranda-Lugo (proc. 88882.379164/2019-01). The technical support for the built-up of the experimental rig given by Mr. Pedro Donizete, and Mr. Lazaro is also appreciated and recognized.

## 6 REFERENCES

- Arrollo Caballero, J. E. (2023). *Caracterização do escoamento horizontal líquido-líquido anular via velocimetria por imagem de partículas (PIV) e fluorescência induzida por laser planar (PLIF)*. [Dissertação de Mestrado]. Universidade de São Paulo.
- Ashwood, A. C., Vanden Hogen, S. J., Rodarte, M. A., Kopplin, C. R., Rodríguez, D. J., Hurlburt, E. T., & Shedd, T. A. (2014). Reprint of: A multiphase, micro-scale PIV measurement technique for liquid film velocity measurements in annular two-phase flow. *International Journal of Multiphase Flow*, 67(S), 200–212. <https://doi.org/10.1016/j.ijmultiphaseflow.2014.10.011>
- Bannwart, A. C. (2001). Modeling aspects of oil-water core-annular flows. *Journal of Petroleum Science and Engineering*, 32(2), 127–143. [www.elsevier.com/locate/jpetscieng](http://www.elsevier.com/locate/jpetscieng)
- Bannwart, A. C., Rodriguez, O. M. H., De Carvalho, C. H. M., Wang, I. S., & Vara, R. M. O. (2004). Flow patterns in heavy crude oil-water flow. *Journal of Energy Resources Technology, Transactions of the ASME*, 126(3), 184–189. <https://doi.org/10.1115/1.1789520>
- Brauner, N. (1991). Two-phase liquid-liquid annular flow. In *Int. J. Multiphase Flow* (Vol. 17, Issue I).
- Elseth, G. (2001). *An Experimental Study of Oil / Water Flow in Horizontal Pipes*.
- Ibarra, R., Matar, O. K., & Markides, C. N. (2021). Experimental investigations of upward-inclined stratified oil-water flows using simultaneous two-line planar laser-induced fluorescence and particle velocimetry. *International Journal of Multiphase Flow*, 135. <https://doi.org/10.1016/j.ijmultiphaseflow.2020.103502>
- Ibarra, R., Zadrazil, I., Matar, O. K., & Markides, C. N. (2018). Dynamics of liquid-liquid flows in horizontal pipes using simultaneous two-line planar laser-induced fluorescence and particle velocimetry. *International Journal of Multiphase Flow*, 101, 47–63. <https://doi.org/10.1016/j.ijmultiphaseflow.2017.12.018>
- Kumara, W. A. S., Halvorsen, B. M., & Melaaen, M. C. (2010). Particle image velocimetry for characterizing the flow structure of oil-water flow in horizontal and slightly inclined pipes. *Chemical Engineering Science*, 65(15), 4332–4349. <https://doi.org/10.1016/j.ces.2010.03.045>
- Rodriguez, O. M. H., & Bannwart, A. C. (2006). Experimental study on interfacial waves in vertical core flow. In *Journal of Petroleum Science and Engineering* (Vol. 54, Issues 3–4, pp. 140–148). <https://doi.org/10.1016/j.petrol.2006.07.007>
- Rodriguez, O. M. H., & Bannwart, A. C. (2008). Stability analysis of core-annular flow and neutral stability wave number. *AIChE Journal*, 54(1), 20–31. <https://doi.org/10.1002/aic.11361>
- Shi, J., & Yeung, H. (2017). Characterization of liquid-liquid flows in horizontal pipes. *AIChE Journal*, 63(3), 1132–1143. <https://doi.org/10.1002/aic.15452>
- Sutharshan, B. , K. M. , O. A. (1995). Measurement of circumferential and axial liquid-film velocities in horizontal annular-flow. *Int. J. Multiph. Flow* , 21, 193–206.
- Zadrazil, I., & Markides, C. N. (2014). An experimental characterization of liquid films in downwards co-current gas-liquid annular flow by particle image and tracking velocimetry. *International Journal of Multiphase Flow*, 67(S), 42–53. <https://doi.org/10.1016/j.ijmultiphaseflow.2014.08.007>
- Zadrazil, I., Matar, O. K., & Markides, C. N. (2014). An experimental characterization of downwards gas-liquid annular flow by laser-induced fluorescence: Flow regimes and film statistics. *International Journal of Multiphase Flow*, 60, 87–102. <https://doi.org/10.1016/j.ijmultiphaseflow.2013.11.008>

## 7 RESPONSIBILITY NOTICE

The authors are the only one responsible for the printed material included in this paper.